



Iron storage capacities and associated ferritin gene expression among marine diatoms

Natalie R. Cohen ¹, Elizabeth Mann,² Brooke Stemple,¹ Carly M. Moreno,¹ Sara Rauschenberg,² Jeremy E. Jacquot,² William G. Sunda,¹ Benjamin S. Twining ²*, Adrian Marchetti¹*

¹Department of Marine Sciences, University of North Carolina at Chapel Hill, Chapel Hill, North Carolina

²Bigelow Laboratory for Ocean Sciences, East Boothbay, Maine

Abstract

In large regions of the ocean, low iron availability regulates diatom growth and species composition. Diatom species often vary in their physiological response to iron enrichment, with natural and artificial iron additions in iron-limited regions of the ocean resulting in large blooms of primarily pennate diatoms. The ability of pennate diatoms to proliferate following pulse iron additions has been partly attributed to their ability to acquire and store excess intracellular iron in the iron storage protein ferritin. Recent transcriptome sequencing of diatoms indicate that some centric diatoms also possess ferritin. Using a combination of physiological and molecular techniques, we examined the iron storage capacities and associated ferritin gene expression in phylogenetically diverse centric and pennate diatoms grown under high and low iron concentrations. There were no systematic differences among ferritin-containing and non-containing diatom lineages in their ability to store iron in excess of that needed to support maximum growth rates. An exception, however, was the ferritin-containing pennate diatom *Pseudo-nitzschia granii*, native to iron-limited waters of the Northeast Pacific Ocean. This species exhibited an exceptionally large luxury iron storage capacity and increased ferritin gene expression at high iron concentrations, supporting a role in long-term iron storage. By contrast, two other diatoms species that exhibited minimal iron storage capacities contained two distinct ferritin genes where one ferritin gene increased in expression under iron limitation while the second showed no variation with cellular iron status. We conclude that ferritin may serve multiple functional roles that are independent of diatom phylogeny.

Diatoms are a critical component of the oceans' biological carbon pump which consists of the photosynthetic fixation of carbon dioxide (CO₂) into organic matter by phytoplankton in the ocean's surface layer and the subsequent transport of this carbon to the deep ocean. This biological pump plays a major role in the regulation of atmospheric CO₂ and hence global climate (Sarmiento and Bender 1994). The strength and efficiency of the biological carbon pump in large areas of the oceans, including the Southern Ocean and the equatorial and subarctic northeast Pacific Ocean, is substantially reduced by the limited availability of the micronutrient iron. Iron inputs from a variety of sources including aeolian transport of continental dust, vertical mixing, inputs from coastal sediments and rivers and active hydrothermal venting are unable to meet the biological demand for iron in these

regions (Moore et al. 2002; Saito et al. 2013). Diatoms typically dominate algal blooms when iron is introduced into iron-limited ocean waters, commonly referred to as high-nutrient, low chlorophyll (HNLC) regions (Boyd et al. 2007). They possess a range of strategies for coping with iron limitation that allow them to persist under low iron conditions and rapidly bloom in response to episodic iron inputs (Sunda and Huntsman 1995; Marchetti et al. 2012). These mechanisms include decreasing metabolic iron demands through a decrease in the abundance of iron-rich photosynthetic protein complexes (Strzeppek and Harrison 2004); replacing iron-containing proteins with alternative iron-free proteins (LaRoche et al. 1995; Peers and Price 2006; Allen et al. 2008; Lommer et al. 2012); the utilization of high affinity iron uptake systems (Maldonado and Price 2001; Shaked et al. 2005; Morrissey and Bowler 2012; Morrissey et al. 2015) and luxury iron uptake (i.e., exceeding what is required to achieve maximum growth rate) through the use of iron storage mechanisms (Sunda and Huntsman 1995; Marchetti et al. 2009).

*Correspondence: amarchetti@unc.edu or btwinning@bigelow.org

Additional Supporting Information may be found in the online version of this article.

Iron storage in some diatoms is achieved through the use of ferritins, a ubiquitous family of proteins found across all domains of life including bacteria, plants, and animals (Theil et al. 2006; Marchetti et al. 2009; Groussman et al. 2015). These proteins store large quantities of intracellular iron, thereby preventing iron toxicity. True ferritins are comprised of 24 subunits and may be up to 480 kDa in size. They can store up to 4500 iron atoms as the insoluble iron oxide ferrihydrate within an inner core nano-cage subunit structure (Liu and Theil 2005). Gated pores control iron flow (as ferrous iron [Fe(II)]) into and out of the inner core (Theil et al. 2008).

One well-characterized role of diatom ferritin is in long-term iron storage (Marchetti et al. 2009). Certain diatoms living in chronically iron-limited environments that receive episodic iron inputs exhibit increased ferritin synthesis following these inputs and are thus able to store large reserves of iron in their ferritins (Marchetti et al. 2009). They then use this stored iron to support subsequent growth when iron levels in the surrounding seawater drop back to low ambient concentrations. This process ensures a steady intracellular supply of iron to support growth and cell division, and is thought to be a major factor contributing to the numerical dominance of mostly ferritin-containing pennate diatoms following iron fertilization events (Marchetti et al. 2009).

In other algal lineages, including the green alga *Chlamydomonas reinhardtii* and *Ostreococcus tauri*, various functional roles for ferritin in microalgae have been described. *C. reinhardtii* contains two distinct ferritin proteins with seemingly different functional roles; one increases in protein expression under high iron conditions, while the other displays the opposite trend and increases expression under iron limitation, potentially serving as an intracellular iron buffer when iron is released from the degradation of iron-containing proteins during iron-induced stress (La Fontaine et al. 2002; Long et al. 2008). In addition, the green alga *O. tauri* has recently been found to exhibit circadian behavior in ferritin expression in which both transcript and protein abundances decrease during the day and subsequently increase at night, perhaps to store internal iron pools during periods of darkness when iron-rich photosynthetic protein complexes are not as abundant (Botebol et al. 2015). Given the variety of observed ferritin responses, it is likely that multiple functional roles for ferritin have evolved across and even within different algal lineages.

The two main lineages of diatoms, centrics and pennates, are estimated to have diverged relatively recently in geologic time—about 90 million years ago; yet they substantially differ in their genetic make-up (Bowler et al. 2008; Armbrust 2009). Pennate diatoms, such as those belonging to the genera *Pseudo-nitzschia* or *Fragilariopsis*, frequently dominate large blooms in iron-limited regions of the ocean following iron enrichment, and outcompete centric diatoms and other phytoplankton groups present in the initial assemblages (de

Baar et al. 2005). This tendency has been partially attributed to their use of ferritin (Marchetti et al. 2009). Although it was initially thought that only pennate diatoms contained ferritin based on a limited number of sequenced diatom genomes, a recent community-wide transcriptomic sequencing effort has provided evidence that some centric diatoms also possess ferritin-like gene homologs (Groussman et al. 2015).

It remains unclear whether centric diatoms that contain ferritin can store iron to a similar extent as ferritin-containing pennate diatoms and whether these centric diatoms depend on ferritin for long-term storage of iron to sustain growth and cell division following episodic iron input events. This study aims to examine whether ferritin-containing vs. non-containing centric and pennate diatoms systematically differ in their iron storage capacities, and whether the two diatom groups differ in their ferritin gene expression in response to varying iron concentrations in their environment. A phylogenetically diverse group of diatoms was cultured under varying iron conditions in order to quantify their iron storage capacities. Our findings provide evidence to support multiple distinct functional roles for ferritin among diatoms that may influence cellular acclimation and adaptation to variations in iron supply and subsequent metabolic utilization.

Materials

Experimental design and diatom culturing methodology

Diatoms used in this study were selected on the basis of phylogeny, the availability of transcriptome sequence information and subsequent presence/absence of a ferritin gene. The pennate diatom, *Pseudo-nitzschia granii* UNC1102, was isolated from the Northeast Pacific Ocean in 2011 (Ocean Station Papa: 50°N, 145°W; Table 1). All other isolates were obtained from the Provasoli-Guillard National Center for Marine Algae and Microbiota (NCMA; East Boothbay, ME, U.S.A.). Cultures of each isolate were grown using the semi-continuous batch culture technique, allowing cells to remain in exponential growth phase throughout the experimental period. All culture work was performed using the synthetic seawater medium Aquil, which was microwave-sterilized before use (Price et al. 1989). The nitrate, phosphate, and silicic acid concentrations were 300 $\mu\text{mol L}^{-1}$, 10 $\mu\text{mol L}^{-1}$, and 100–200 $\mu\text{mol L}^{-1}$, respectively. Trace metals were buffered with 100 $\mu\text{mol L}^{-1}$ ethylenediaminetetraacetic acid (EDTA) and the B-vitamins cyanocobalamin, biotin, and thiamine were supplied. Total iron was added as FeEDTA chelates. Trace metal clean techniques were implemented while preparing the Aquil medium and during handling of cultures (Marchetti et al. 2015). All prepared Aquil media were allowed to equilibrate overnight before experimental use. Cultures were grown at 12°C, 14°C, or 20°C depending on their habitable ranges as provided by the NCMA or based on

Table 1. Diatom isolation locations, growth temperatures, biovolumes, and growth rates within culture experiments. Maximum growth rates (μ_{\max}) within the experimental high iron treatment were obtained using iron concentrations in excess of that needed to achieve maximum iron-saturated growth (1370 nmol L⁻¹ total iron [Fe_T]). The low iron treatment concentrations were intended to target near-maximum iron-saturated growth states (1.5–600 nmol L⁻¹ Fe_T, see “Methods” section). The growth rates presented correspond to gene expression culture experiments for isolates containing a *FTN* homolog, and correspond to iron quota culture experiments for all other isolates. Relative growth rates of isolates containing a *FTN* homolog within iron quota culture experiments are presented in Fig. 2. The number of distinct *FTN* homologs identified within each isolate’s transcriptome are displayed. ND = none detected.

Isolate (strain ID)	Isolation location	Diatom lineage	Biovolume (μm^3)	Temperature (°C)	μ_{\max} (d ⁻¹)	$\mu \mu_{\max}^{-1}$ [low iron]	<i>FTN</i> copies
<i>Pseudo-nitzschia granii</i> (UNC1102)	Northeast Pacific 50°N 145°W (oceanic)	Raphid pennate	46 ± 11	12	1.27 ± 0.07	0.77 ± 0.07	1
<i>Amphora coffeaeformis</i> (CCMP127)	North Atlantic 41.5°N 70.7°W (coastal)	Raphid pennate	500 ± 191	20	1.64 ± 0.31	0.50 ± 0.11	2
<i>Thalassionema frauenfeldii</i> (CCMP1798)	North Atlantic 18.5°N 64.6°W (coastal)	Araphid pennate	1305 ± 798	20	0.65 ± 0.03	0.78 ± 0.05	2
<i>Grammatophora oceanica</i> (CCMP410)	South Pacific 37.9°S 144.9°E (coastal)	Araphid pennate	860 ± 273	20	0.31 ± 0.06	0.9 ± 0.26	ND
<i>Minutocellus polymorphus</i> (CCMP3303)	South Atlantic 17.5°S 11.25°E (coastal)	Bipolar centric	188 ± 65	20	1.84 ± 0.12	0.78 ± 0.23	1
<i>Thalassiosira</i> sp. (NH16)	North Pacific 45.7°N 124.5°W (coastal)	Bipolar centric	332 ± 144	20	0.51 ± 0.04	0.51 ± 0.12	1
<i>Thalassiosira rotula</i> (CCMP3096)	North Pacific 49.7°N 127.4°W (coastal)	Bipolar centric	7525 ± 3609	14	0.38 ± 0.08	0.82 ± 0.20	2
<i>Thalassiosira weissflogii</i> (CCMP1336)	North Atlantic 41.1°N 72.1°W (coastal)	Bipolar centric	741 ± 195	20	1.26 ± 0.06	0.81 ± 0.05	ND
<i>Thalassiosira pseudonana</i> (CCMP1335)	North Atlantic 40.8°N 72.8°W (coastal)	Bipolar centric	93 ± 70	20	1.49 ± 0.23	0.82 ± 0.15	ND
<i>Thalassiosira oceanica</i> (CCMP1005)	North Atlantic 33.2°N 65.3°W (oceanic)	Bipolar centric	149 ± 59	20	1.14 ± 0.04	0.63 ± 0.03	ND
<i>Corethron hystrix</i> (CCMP308)	North Atlantic 58.5°N 0.3°W (coastal)	Radial centric	19,309 ± 5695	14	0.56 ± 0.03	0.5 ± 0.14	ND

the location of isolation (see Table 1). Diatoms were grown under continuous light at an intensity of 110–150 $\mu\text{mol quanta m}^{-2} \text{ s}^{-1}$, except for *Thalassionema frauenfeldii* which was grown under a 13/11 light/dark cycle due to an inability to grow under continuous light conditions. Growth rates, gene expression, and iron quotas for this isolate were all obtained during the light period. Growth rates were determined from in vivo chlorophyll *a* fluorescence, monitored with a Turner Designs 10-AU fluorometer, and calculated from linear regression of the natural log of fluorescence vs. time (Brand et al. 1981). Isolate size dimensions were estimated using light microscopy (Leica DMI6000). Lengths and widths of 9–17 individual cells were measured and incorporated into calculations to determine biovolume (μm^3) from approximate geometric microalgal shapes (Hillebrand et al. 1999).

All cultures were grown at two iron concentrations. The high concentration (1370 nmol L⁻¹ total iron [Fe_T]) was well in excess of that needed to achieve a maximum iron-

saturated growth rate (μ_{\max}). Diatoms were also grown at a low iron concentration (1.5–600 nmol L⁻¹ depending on the species) in which the growth was mildly to moderately iron-limited. Cultures were acclimated to their high and low iron conditions for a minimum of three transfers, undergoing approximately 15–20 cell divisions, before measurement of gene expression and iron quotas. For measurement of these two parameters, separate cultures were grown concurrently; however, the two sets of cultures for *Amphora coffeaeformis* and *T. frauenfeldii* had to be grown at independent institutions and show some differences in iron limitation results (see Table 1 and Fig. 2).

Cellular iron quotas

Iron quotas normalized to carbon (Fe : C) were obtained by growing triplicate cultures at high and low iron concentrations using the ⁵⁵Fe/¹⁴C dual labeling approach (Twining et al. 2004; Marchetti et al. 2006). The specific activity of the ⁵⁵Fe stock was 549 $\mu\text{Ci } \mu\text{mol}^{-1}$ for *Pseudo-nitzschia* cultures,

and $392 \pm 11.3 \mu\text{Ci } \mu\text{mol}^{-1}$ for the remainder of the isolates. Cultures were grown in 28 mL polycarbonate centrifuge tubes that had been acid-cleaned and rinsed with Milli-Q water. For high iron media, 1% of Fe_T was added as radiolabeled $^{55}\text{FeCl}_3$ with the remaining 99% consisting of non-labeled FeCl_3 , while in the low iron media 15–100% of the total iron consisted of radiolabeled $^{55}\text{FeCl}_3$ with the remainder added as unlabeled FeCl_3 . Approximately 2 nanoCi of $\text{H}^{14}\text{CO}_3^-$ was added to each 28 mL iron treatment to allow for measurement of cellular fixed carbon. Radiolabeled media were allowed to equilibrate for 24 h before inoculation with cells. Cultures were harvested when they reached mid- to late-exponential phase, allowing for approximately five cell divisions. Cells were filtered onto 47 mm polycarbonate filters (3 μm pore size) and were subsequently exposed to a titanium/citrate EDTA solution for 5 min to reduce extracellular Fe(III) to Fe(II) and thereby removes iron oxyhydroxides and iron adsorbed to cell surfaces (Tang and Morel 2006). The ^{14}C activity of filters rinsed with seawater and with the titanium/citrate EDTA reducing solution was similar, except for *Corethron hystrix* which lost an average of $61\% \pm 0.1\%$ of its measured cellular carbon concentration after exposure to the reducing solution. The filters were transferred to scintillation vials and cellular ^{55}Fe and ^{14}C were determined via liquid scintillation counting with a dual-label protocol (Beckman). Cell associated ^{55}Fe and ^{14}C activity was corrected for filter blanks by subtracting counts on filters through which cell-free culture media had been passed. Cell-free blanks were on average $< 10\%$ of the total activity, with the exception of ^{14}C in *C. hystrix* in the low iron treatment where the blank represented 55% of the total activity, possibly due to the loss of carbon from the cells during the titanium/citrate EDTA rinse. The ratio of ^{55}Fe to ^{14}C disintegrations per minute was 2.56 ± 0.94 for low iron cultures and 6.70 ± 2.37 for high iron cultures.

To distinguish between the amount of luxury stored iron and metabolic iron needed to support cellular growth at the high, growth-saturating iron concentration, the amount of metabolic iron must be determined. This was estimated from the specific growth rate and cellular iron quota in the iron-limited, low iron cultures by assuming a linear relationship between iron-limited growth rate and cellular iron quota, as has been previously observed (Sunda and Huntsman 1997; see Supporting Information Methods; Supporting Information Figs. S1, S2). The estimated cellular iron quotas needed to support the observed μ_{max} (rather than the measured iron quotas in the low iron conditions) were then subtracted from the cellular iron quotas measured at high iron concentrations ($1370 \text{ nmol L}^{-1} \text{ Fe}_T$) to yield estimates of luxury iron uptake and storage ($\text{Fe-Q}_{\text{Store}}$). These values reflect the ability of the diatom species to take up iron at high external iron concentrations exceeding that required to support maximum growth rate. An exception was *Thalassiosira oceanica* where the minimum iron quota needed to support μ_{max} was

estimated from previously reported iron quotas and specific growth rates (Marchetti et al. 2006). Although a few of the isolates in our study did not experience significant reductions in growth rates between the high and low iron treatments (see Fig. 2) we speculate that any further iron limitation would not have resulted in substantial reductions in iron quotas or caused an appreciable change in our estimated $\text{Fe-Q}_{\text{Store}}$ values due to the quotas obtained under high iron conditions having a much stronger influence on $\text{Fe-Q}_{\text{Store}}$ (see Supporting Information Methods).

Target gene sequence acquisition and phylogenetic analysis

P. granii ferritin (*FTN*) and actin (*ACT*) gene sequences were retrieved from a previously sequenced transcriptome library (accession number SRX0066451; Marchetti et al. 2012). *ACT* was chosen as the reference gene to determine relative gene expression due to its constitutive expression under a variety of growth conditions (Alexander et al. 2012). Gene sequences for *FTN* and *ACT* from the isolates examined in this study were obtained through a sequence homology search using BLASTx v2.2.28 with *P. granii* genes against the database Marine Microbial Eukaryote Transcriptome Sequencing Project (MMETSP) using an e-value cutoff of 10^{-5} (Altschul et al. 1990). In addition, *Pseudo-nitzschia multiseriis* and *Fragilariopsis cylindrus* protein sequences used in the *FTN* phylogenetic tree were acquired from the publicly available JGI Genome Portal. Paired-end *FTN* read counts of the transcriptomes of MMETSP isolates in this study ranged from 277 to 1472 with a mean of 607, indicating that the gene is likely to be present at transcript levels substantial enough to be detected under iron-replete conditions (iMicrobe, MMETSP). Nevertheless it is possible that transcriptome sequencing depth did not capture the presence of *FTN* in the isolates where a *FTN* gene homolog was not identified. Therefore the assumption that the non-ferritin-containing diatom isolates used in this study are truly without ferritin must be interpreted with caution. It may be important to note that alternative sequence search methodology may uncover additional *FTN* copies present in transcriptomes unidentified by the search tools and settings used here.

For phylogenetic analysis, *FTN* sequences within the open reading frame were aligned using MUSCLE within Geneious v5.6.4 software (Edgar 2004). A Maximum-Likelihood tree was created with MEGA6 using the JTT matrix-based model, partial deletion of residues and 100 bootstrap replicates (Tamura et al. 2013). Diatoms were grouped into classes (i.e., raphid pennate, araphid pennate, bi-multipolar centric, or radial centric) based on chronograms from Sorhannus (2007).

Primer development, RNA extraction, and gene expression

Primers were designed for each examined *FTN*-containing diatom individually using Primer3 v0.4.0 (Supporting

Information Table S1, Untergasser et al. 2012), tested via PCR and visualized through gel electrophoresis. Correct target amplification was confirmed through Sanger sequencing of the resulting PCR product. For RNA analysis, triplicate 500 mL cultures were grown in polycarbonate bottles that were autoclaved, acid-cleaned and Milli-Q rinsed. Cultures were harvested onto 25 mm or 47 mm polycarbonate filters (3 μm pore size) in mid- to late-exponential growth phase to achieve adequate biomass. Filters were flash frozen in liquid nitrogen and then stored at -80°C until RNA extraction. RNA extractions were performed using the RNAqueous 4-PCR kit (Ambion) followed by DNAsing at 37°C for 45 min with DNase I (Ambion) according to the manufacturer's guidelines. Up to 2 μg of total RNA was reverse transcribed to cDNA, or all of the total RNA obtained if the extracted yield was lower, using the SuperScript III First-Strand cDNA Synthesis kit with oligo-dt primers (Invitrogen). Real-time quantitative PCR (qPCR) was performed on synthesized cDNA with a Mastercycler ep realplex² (Eppendorf).

Relative gene expression of *P. granii* *FTN* normalized to *ACT* was estimated using two distinct methods. First, the ΔCt method [$2^{-(\Delta\text{Ct})}$] (Pfaffl 2001), and second, using a series of standards for each gene ranging from 10 to 10^6 copies μL^{-1} (Marchetti et al. 2015; Ellis et al. 2017). The validity of the ΔCt method was supported by comparison to the standard curve method for *P. granii*. Relative gene expression obtained through either method was found to be similar (Supporting Information Fig. S3) and therefore the *FTN* gene expression analysis of the other isolates was performed using the ΔCt method.

Quantitative-PCR reaction protocols closely follow those outlined by Marchetti et al. (2015), with 20 μL triplicate reactions consisting of a 2 μL cDNA template, 10 μL KAPA SyberFast qPCR kit mix (Kapa), 1.6 μL forward and reverse primers (0.8 $\mu\text{mol L}^{-1}$ each), and 4.8 μL of UV-light treated milli-Q water. For the creation of *P. granii* *FTN* and *ACT* standards, target DNA sequences were amplified by PCR at 94°C for 2 min, followed by 40 cycles for 30 s at 95°C , 30 s at the optimum annealing temperature specific to each primer set, and 1 min at 72°C . PCR cocktail reactions consisted of 4 μL DNA template, 2 μL MgCl_2 , 2 μL of Taq buffer (Promega), 0.8 μL of the forward and reverse primers, 0.15 μL Taq polymerase (Promega), and 9.25 μL of UV-light treated milli-Q water (Marchetti et al. 2015). Amplified products were transformed into competent *E. coli* cells using the TOPO TA Cloning Kit (Invitrogen). Kanamycin-resistant colonies containing the inserted vector and fragment were grown overnight in Luria Broth and plasmids were extracted using QIAprep Miniprep (Qiagen). Plasmids were linearized using the enzyme *Spe I* at 37°C for 1 h, followed by 20 min at 80°C . Qubit RNA Assay Kit (Invitrogen) was used to quantify linearized plasmid and standards were created by diluting to 10– 10^6 copies μL^{-1} . To test for statistical differences in gene expression between iron

treatments, a one-way analysis of variance (ANOVA) was performed. Data sets were tested for normality, equal variance and a Holm-Sidak or Tukey pairwise multiple comparison test was performed using Sigmaplot 12.5. The level of significance was $p < 0.05$.

Biogeographical distribution of ferritin possession

An assessment of the biogeographical distribution of diatom ferritin gene homologs was conducted for all isolates with sequenced transcriptomes and isolation location information. In addition to *P. granii* and diatoms sequenced as part of MMETSP, eight polar diatoms isolated from the Western Antarctica Peninsula region were also included (Moreno et al. 2017). MMETSP strain isolation locations, when available, were retrieved from either the MMETSP iMicrobe database or the NCMA website. All isolate locations were plotted using a custom MATLAB script. Annual mean surface nitrate concentrations were obtained from the World Ocean Atlas 2009 (Garcia et al. 2010). Fisher's exact test was used to compare the distribution of *FTN* that were present or absent in diatoms isolated from HNLC regions and non-HNLC regions (equatorial Pacific, Northeast Pacific, and Southern Ocean; Moore et al. 2002), of which the Southern Ocean was the only location with an adequate number of diatoms with sequenced transcriptomes.

Results

Ferritin phylogenetic analysis of centric and pennate diatoms

The recent transcriptome sequencing of 78 diatoms as part of MMETSP has provided an opportunity to determine the prevalence of ferritin throughout the diatom lineage. Through querying this database, along with additional publicly available diatom transcriptomes and genomes, we found that over 85% of the sequenced pennate diatoms contain at least one *FTN* homolog compared to 41% of centric diatoms (Fig. 1A). The majority of ferritin-containing diatoms within the database are pennates (62% pennates vs. 38% centrics), despite centric diatoms making up the majority of sequenced isolates (44 centrics vs. 34 pennates).

Within the centric diatom lineage, bi-multipolar diatoms are better represented than radial centrics, and the majority of them (65%) do not contain a *FTN* homolog. Roughly half of the radial centrics contain a *FTN* homolog within their transcriptomes. The pennate lineage is mostly represented by raphid as compared to araphid pennates, of which all but one (*Stauroneis constricta* or 96% of the total) contain at least one *FTN* homolog. Similarly, most araphid pennate diatoms (67%) contain *FTN*.

The high number of diatom transcriptome sequences also provided the opportunity to examine the phylogenetic relatedness of *FTN* within this algal group. Centric and pennate diatoms do not form exclusive subgroups that are commonly observed through phylogenetic analysis of evolutionarily

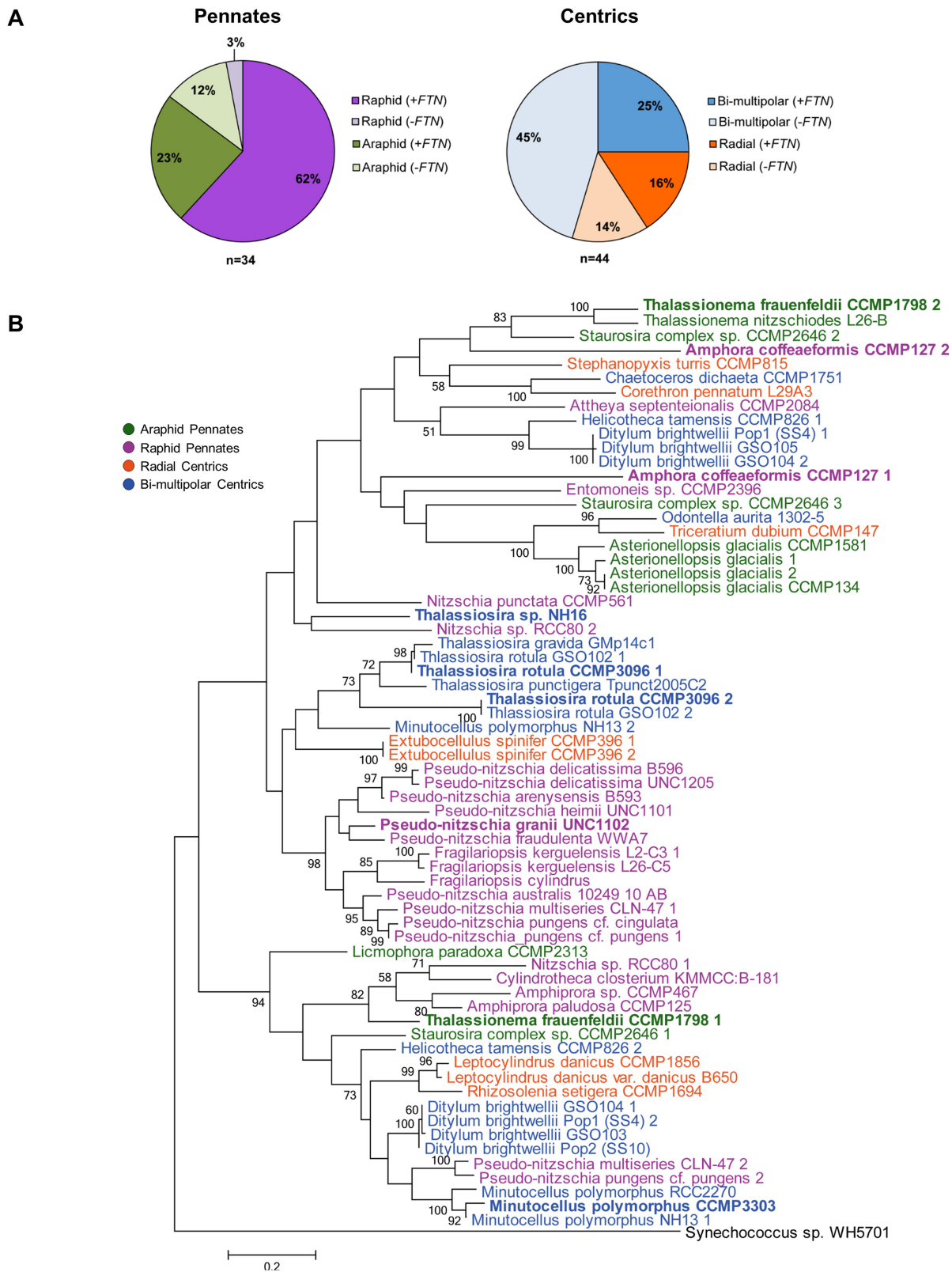


Fig. 1. (A) *FTN* presence and absence within MMETSP transcriptomes. The pennate diatom classes, Bacillariophyceae (raphid) and Fragilariophyceae (araphid) are shown in purple and green, respectively, while the centric diatom classes, Mediophyceae (bi-multipolar) and Coscinodiscophyceae (radial) are shown in blue and orange, respectively. Darker colors represent fractions of species within the transcriptome database containing *FTN*, while lighter shades of colors indicate proportions of diatom species without an identified *FTN* homolog. **(B)** Maximum-Likelihood tree of *FTN* among the four classes of diatoms. Numbers beside nodes indicate bootstrap values; only bootstraps above 50 are included. *Synechococcus* sp. WH5701 was used as the outgroup. Strains examined in this study are indicated in bold. Isolates containing *FTN* but excluded from the tree due to only partial amino acid sequences available include *Chaetoceros neogracle* CCMP1317, *Fragilariopsis kerguelensis* L2-C3, *Thalassiothrix antarctica* L26-D1, and *Synechococcus recta* CCMP1620.

conserved genes such as those of ribosomal RNA (e.g., 18S rDNA). Rather, distinct clades exist consisting of mixtures from both diatom lineages and all four subgroups (Fig. 1B). Additionally, some diatom strains contained more than one *FTN* homolog (Fig. 1B: denoted with 1 and 2 following strain ID). These ferritins varied in degree of similarity, from being quite distinct and located in different clades within the phylogenetic tree (e.g., *T. frauenfeldii* CCMP1798 1 and 2), to being similar and clustering closely together (e.g., *Thalassiosira rotula* CCMP3096 1 and 2).

Iron storage capacities among diatoms

Among the diatom isolates examined, μ_{\max} under high-iron conditions varied fourfold within the iron quota culture experiments, ranging from a high of $1.9 \pm 0.14 \text{ d}^{-1}$ in *Minutocellus polymorphus* to $0.45 \pm 0.02 \text{ d}^{-1}$ in *T. rotula* (Supporting Information Fig. S1). In the iron quota experiments, growth rates decreased by an average of 20% in the low iron cultures relative to maximum growth rates in high iron cultures, indicating mild to moderate iron limitation in most isolates regardless of biovolume (Fig. 2; Supporting Information Fig. S4). These values were overall consistent with results in the gene expression culture experiments, where the growth rate of the iron-limited cultures were an average of 31% lower than the values in high iron cultures (see below; Fig. 2; Table 1). The diatom *T. frauenfeldii* was an exception in that it showed no significant decrease in growth rate in the low iron culture grown for iron quota determination (Fig. 2), in contrast to the 20% reduction observed in the cultures grown for gene expression analysis at the same low iron concentration (Table 1). However, this isolate demonstrated a 60% lower iron quota under low vs. high iron conditions (4 ± 0.8 vs. 10.3 ± 3.4).

Under high iron conditions, the cellular Fe : C ratios in the experimental diatoms varied by over 30-fold, from $10 \pm 3.4 \mu\text{mol Fe mol C}^{-1}$ in the coastal pennate diatom *T. frauenfeldii* to $300 \pm 68 \mu\text{mol Fe mol C}^{-1}$ in the oceanic pennate diatom *P. granii* (Figs. 2, 3). Under the-low iron conditions, minimum iron quotas varied by 10-fold, from $4 \pm 0.8 \mu\text{mol Fe mol C}^{-1}$ in *T. frauenfeldii* to $41 \pm 6 \mu\text{mol Fe mol C}^{-1}$ in *C. hystrix* (Fig. 2). However as noted previously, this species showed an average 61% loss of cellular carbon after treatment of the cells with the titanium-EDTA citrate wash. Iron, on the other hand should be primarily associated with intracellular membranes (e.g., chloroplast membranes), and thus, would be less likely than carbon to be lost from leaky or ruptured cells. Thus these Fe : C values may be erroneously high due to this loss of cellular carbon, most likely from leakage from the cells' cytosol.

Based on the iron quota measurements, the largest estimated "luxury" uptake of iron in excess of that needed to support maximum growth rate ($\text{Fe-Q}_{\text{Store}}$) was achieved in *P. granii* ($293 \mu\text{mol Fe mol C}^{-1}$), with the next largest value measured in *T. oceanica* ($110 \mu\text{mol Fe mol C}^{-1}$; Fig. 3).

The smallest $\text{Fe-Q}_{\text{Store}}$ values (6.3 and $13.7 \mu\text{mol Fe mol C}^{-1}$) were observed in *T. frauenfeldii* and *A. coffeaeformis*, respectively. There were no apparent differences in the $\text{Fe-Q}_{\text{Store}}$ between *FTN*-containing and non-containing centric and pennate diatoms (Fig. 3). Rather, *P. granii* exhibited the largest $\text{Fe-Q}_{\text{Store}}$ due to a combination of having the highest Fe : C under high-iron conditions and one of the lowest estimated Fe : C ratios needed to achieve μ_{\max} (Supporting Information Fig. S1).

Ferritin gene expression as a function of iron status

Trends in *FTN* expression in response to iron status significantly differed among the diatoms regardless of growth rate reduction (Fig. 3). In *P. granii*, the species with the highest $\text{Fe-Q}_{\text{Store}}$ value, the expression of its single *FTN* gene increased by 100-fold with increasing iron quota between the low-iron and high-iron cultures (ANOVA: $p = 0.006$; Fig. 3). Similarly, expression of the single *FTN* gene in *Thalassiosira* sp. NH16 increased with higher cellular iron quota, but only by twofold (ANOVA: $p = 0.01$), much lower than observed in *P. granii*. This lower increase in *FTN* expression was associated with a lower $\text{Fe-Q}_{\text{Store}}$ value than in *P. granii*, but the value was still the third highest observed among the experimental species (Fig. 3). The opposite iron-response pattern was observed in one of the two *FTN* genes in the coastal diatoms *A. coffeaeformis* and *T. rotula*. In these genes, *A. coffeaeformis* (*FTN1*) and *T. rotula* (*FTN2*), *FTN* expression was 1.8- and 160-fold higher under low iron conditions when cellular Fe : C quotas were reduced to growth limiting values (ANOVA: $p = 0.024$ and 5×10^{-5} , respectively; Fig. 3). However, the second *FTN* gene in both species was constitutively expressed and showed no appreciable change with variations in iron growth status and cellular iron quota. It is unlikely that *FTN* expression levels increased linearly with iron stress in these isolates given that *T. rotula* experienced an 18% reduction in growth rate under low iron conditions (Table 1), but displayed a 160-fold increase in *FTN2* expression while the growth rate of *A. coffeaeformis* was reduced by 50% in the low iron culture, but this species exhibited a more modest 1.8-fold increase in relative *FTN1* expression. In *M. polymorphus* and *T. frauenfeldii*, variations in iron quotas and iron limitation of growth rate had no significant effect on the expression of their single *FTN* genes (ANOVA: $p > 0.05$).

In order to examine whether *FTN* expression is affected by other growth conditions, expression was determined for *P. granii* cultures grown under varying iron conditions, light levels, and phases of growth in batch cultures (see Marchetti et al. 2017 for details on experimental design). Here, *FTN* expression was affected primarily by iron status and was mostly unaltered by light-limitation or growth phase (i.e., exponential vs. stationary) (Supporting Information Fig. S5). These results demonstrate that decreased *FTN* expression is not simply a function of growth rate reduction or a general response to resource limitation.

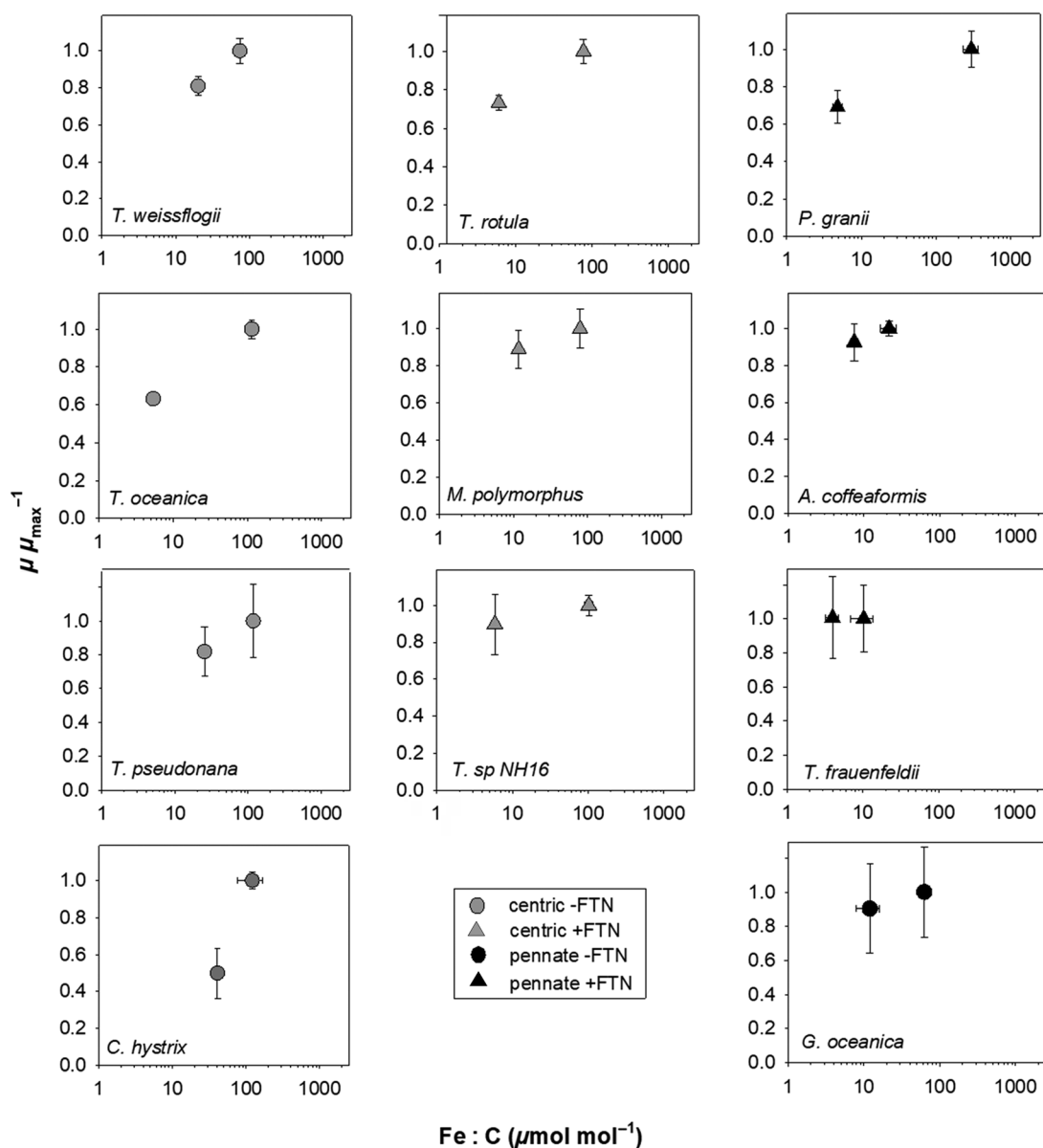


Fig. 2. Ratio of growth rate under low iron conditions ($1.5\text{--}600 \text{ nmol L}^{-1} \text{ Fe}_T$) to maximum growth rate under high iron conditions (μ_{\max}^{-1} ; $1370 \text{ nmol L}^{-1} \text{ Fe}_T$) plotted as a function of the intracellular iron quotas ($\text{Fe} : \text{C}$) for each diatom isolate. Shown are data for pennate (black symbols) and centric (gray symbols) diatoms where at least one *FTN* gene homolog was present (triangles) or absent (circles) in their transcriptomes. Error bars represent the standard deviation of triplicate cultures. *T. oceanica* growth rates and iron quotas are displayed from Marchetti et al. (2006).

Biogeographical analysis of ferritin among diatoms

Diatom isolates used in the analysis of *FTN* distributions were from tropical to polar regions, with the majority obtained from temperate coastal waters (Fig. 4). Many bi-multipolar centrals containing *FTN* were isolated from the northwest coast of the U.S., including *Thalassiosira* sp. NH16 and *T. rotula*. There were no significance differences in *FTN* presence between HNLC and non-HNLC pennate or centric diatoms (Fig. 4; $p \geq 0.5$) with 57% of sequenced diatoms from HNLC regions containing at least one *FTN* gene and 51% from other regions also containing one or more *FTNs* (Fig. 4).

These trends are mainly based on diatom *FTN* presence and absence within the Southern Ocean, the primary HNLC region with sequenced transcriptomes (Fig. 4). For the other iron-limited HNLC regions (e.g., northeast Pacific and equatorial Pacific Oceans) there were too few isolates to draw any definite conclusions on the distribution of *FTN* genes (all raphid pennates). While *P. granii* UNC1102 and *P. heimii* UNC1101 from the northeast Pacific Ocean both contain a *FTN* homolog, the gene was absent from the transcriptome of the equatorial Pacific Ocean diatom *S. constricta* CCMP1120.

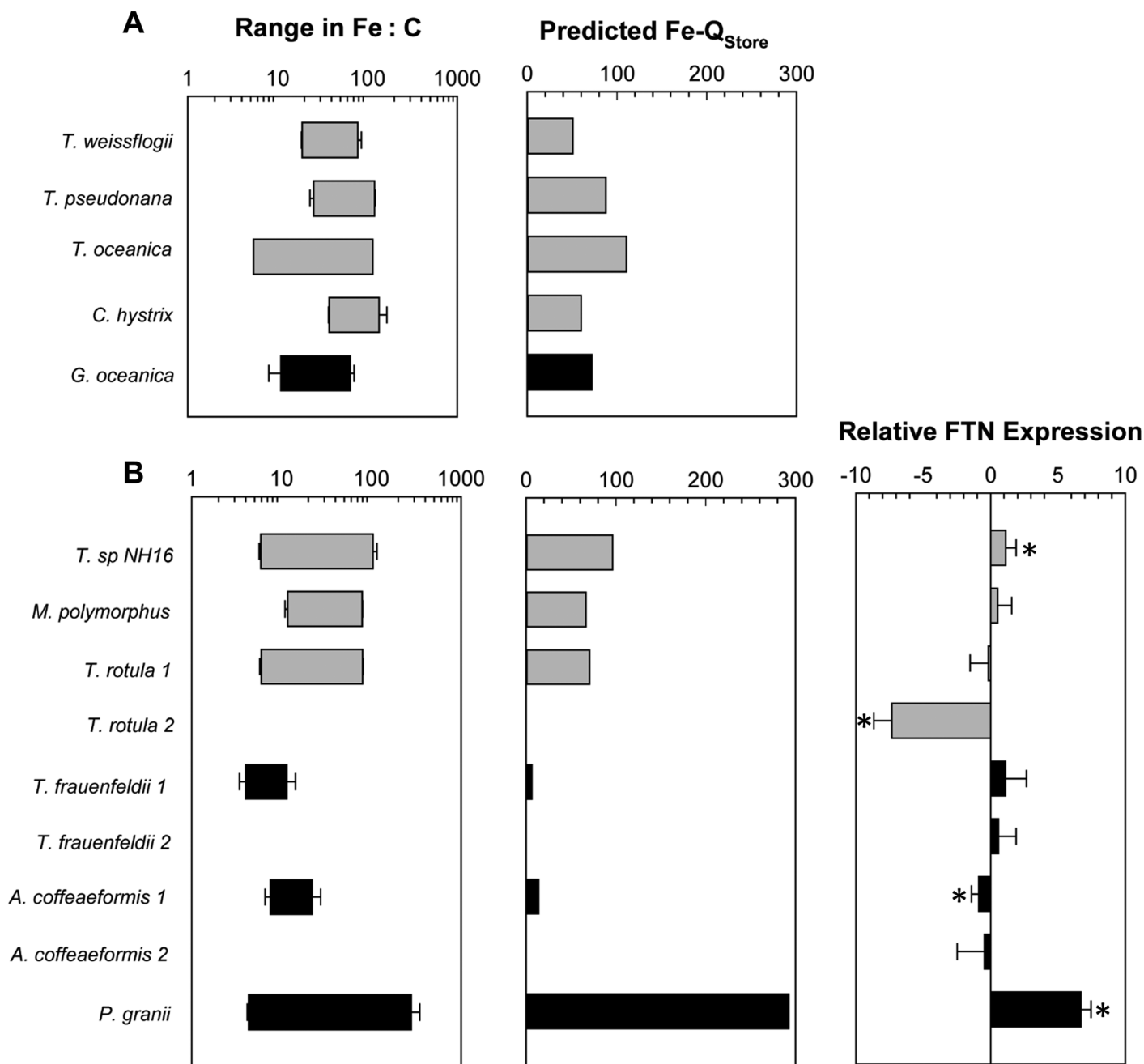


Fig. 3. Comparison of intracellular iron quota (Fe : C) ranges empirically measured, estimated luxury iron storage (Fe-Q_{Store}), and relative *FTN* expression among phylogenetically distinct diatom isolates grown under high and low iron conditions. Diatoms are separated by whether a *FTN* gene is **(A)** absent or **(B)** present within their transcriptomes. Pennate diatoms are displayed in black, centrics in gray. Bar plots display ranges in Fe : C ratios ($\mu\text{mol Fe mol C}^{-1}$) depicted on a log (base 10) scale. The estimated Fe-Q_{Store} displayed on a linear scale are calculated by subtracting empirically measured iron quotas under high iron conditions by estimated iron quotas at μ_{max} (Sunda and Huntsman 1997; see Supporting Information “Methods” section). *T. oceanica* iron quota measurements are from Marchetti et al. (2006). Relative *FTN* expression represents the ratio of actin-normalized *FTN* expression under the high iron conditions compared to the expression under low iron conditions shown on a log (base 2) transformed scale. Multiple *FTN* copies are denoted by 1 and 2. Standard error bars represent variation among triplicate cultures. Positive values indicate a higher number of *FTN* transcripts under high iron conditions, while negative values indicate higher *FTN* expression under low iron conditions. An asterisk (*) indicates a significant statistical difference ($p < 0.05$) in gene expression between high and low iron conditions.

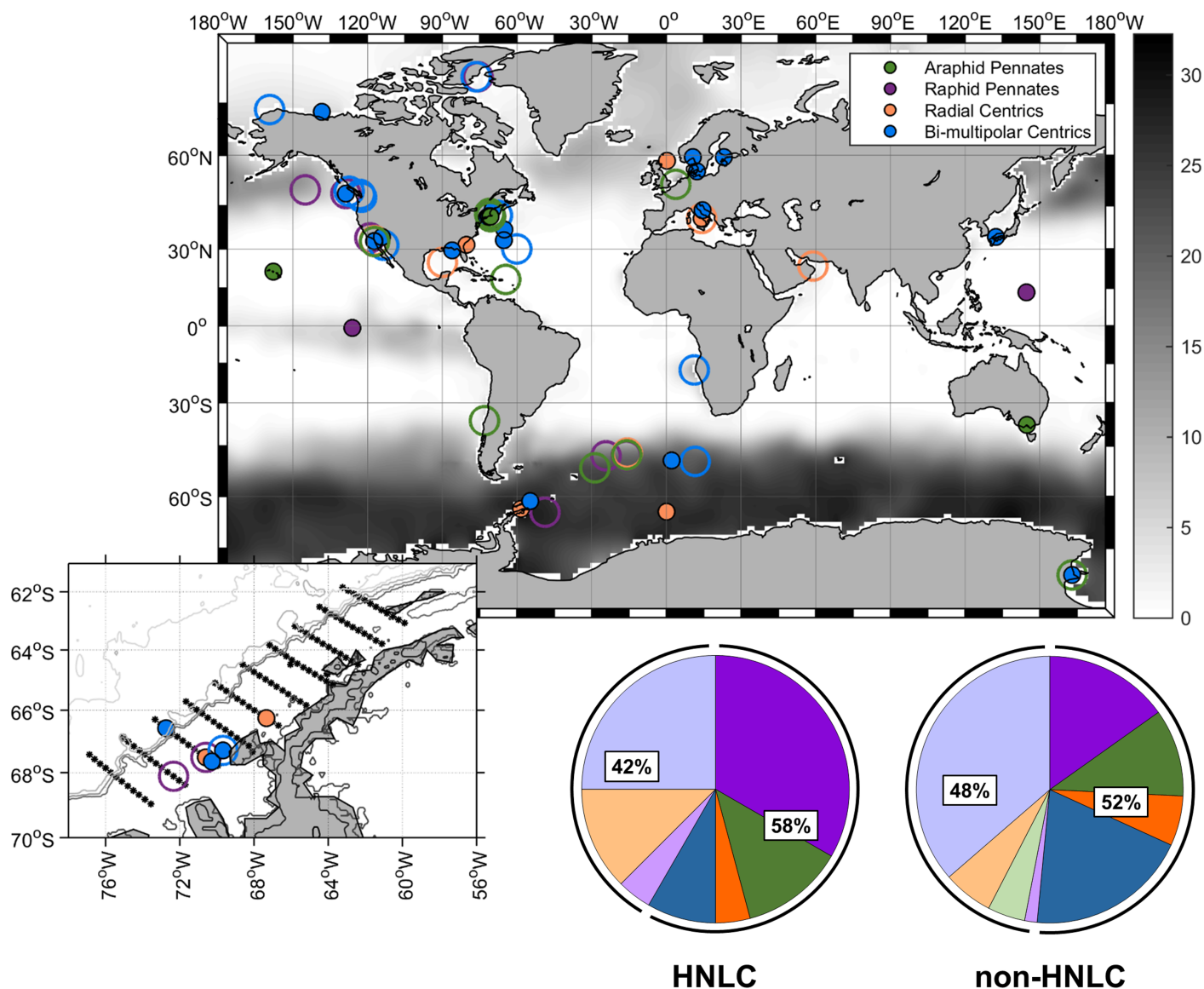


Fig. 4. Global distribution of diatom strains where a *FTN* homolog is present (open circles) or absent (closed circles) within available MMETSP diatom transcriptome sequences. Background grayscale variation represents mean annual surface nitrate concentrations ($\mu\text{mol L}^{-1}$ World Ocean Atlas; [Garcia et al. 2010]). Inset displays the Western Antarctic Peninsula region with the Palmer Long Term Ecological Research (LTER) grid where additional sequenced diatom isolates not contained within MMETSP were obtained. Pie charts represent percentage of isolates within the HNLC vs. non-HNLC regions containing *FTN* or having no *FTN* sequence identified within their transcriptomes. The pennate diatom classes, Bacillariophyceae (raphid) and Fragilariophyceae (araphid) are shown in purple and green, respectively, while the centric diatom classes, Mediophyceae (bi-multipolar) and Coscinodiscophyceae (radial) are shown in blue and orange, respectively. Darker colors represent fractions of isolates containing *FTN*, while lighter corresponding shades indicate proportions without an identified *FTN* homolog. Diatom cultures used for transcriptomes included within MMETSP were primarily grown under iron-replete conditions, and therefore isolates containing ferritin genes that are exclusively expressed under iron limitation may not be identified.

Discussion

Iron storage in diatoms

Our study verifies that centric and pennate diatoms display varied capacities to store iron irrespective of whether they contain ferritin. This complements previous studies showing that diatoms such as *Thalassiosira weissflogii* and *Thalassiosira pseudonana*, which do not contain ferritin,

perform luxury iron uptake at high iron concentrations (Sunda and Huntsman 1995; Nuester et al. 2012). In addition to ferritin, iron may be stored in vacuoles through its incorporation into polyphosphates, as has been demonstrated in yeast (Raguzzi et al. 1988). This may also be true for diatoms. Furthermore, natural resistance associated macrophage proteins (NRAMPs), which transfer divalent metals

(including ferrous iron) out of vacuolar storage in plants, are highly expressed in iron-limited *T. pseudonana* (Lanquar et al. 2005; Kustka et al. 2007), consistent with transport of iron out of vacuoles as an alternative iron storage mechanism to ferritin in diatoms.

In the present study, alternative iron storage mechanisms in the diatoms that do not contain ferritin allowed for similar maximum iron quotas as those achieved in most of the ferritin-containing diatoms under very high iron conditions, demonstrating possession of ferritin alone does not confer an overall enhanced ability to store high levels of non-metabolic cellular iron (Fig. 3). Furthermore, *T. frauenfeldii* contained the lowest estimated luxury iron storage capacity under high iron conditions ($6.3 \mu\text{mol Fe mol C}^{-1}$; Fig. 3B) despite containing two distinct *FTN* genes. Both the identity of these alternative iron storage mechanisms and the mechanisms that regulate the transfer of iron between storage pools and functional iron proteins remain unclear at present. Most importantly, because our experiments were conducted under acclimated growth conditions, it is unclear how the efficacy of ferritin-mediated iron storage compares to non-ferritin iron storage mechanisms during rapid transitions between conditions of low and high iron availability.

Biogeographical patterns in ferritin acquisition

Within the examined diatoms, there were no apparent differences in the luxury iron storage capacities between ferritin-containing and non-ferritin containing diatoms when grown under the same high iron concentrations. What did become apparent was the exceptional iron storage capacity of *P. granii*. A large quota at high iron concentrations combined with a low cellular iron quota needed to achieve μ_{max} resulted in a remarkable capacity of *P. granii* to store iron in excess of that needed to support growth. The ability for continued growth on stored iron supports previous claims as to how iron storage mediated through ferritin likely contributes toward the success of this diatom genera in dominating large blooms in HNLC regions following experimental iron enrichment (Marchetti et al. 2009).

The ability of *P. granii* to substantially decrease the cellular iron needed to support relatively fast growth rates highlights how well adapted this species is to growing in the iron-limited region from which it was isolated. To gain a biogeographical perspective on diatom *FTN* distributions and determine whether possession of ferritin preferentially occurs in diatoms residing in HNLC regions, we searched sequenced transcriptomes of diatoms isolated from throughout the oceans, taking advantage of the geographical coverage offered by isolates sequenced as part of MMETSP (Keeling et al. 2014). Both HNLC and non-HNLC diatoms possess *FTN* transcripts, and it appears to be common throughout the world's oceans with no clear biogeographical pattern associated with its presence in diatoms. This suggests that

ferritin may serve a beneficial role in both environments experiencing chronic low iron conditions and in regions with higher, but perhaps more variable iron levels, such as coastal upwelling regions. Although not addressed in this study, there may be a positive relationship between the presence of ferritin in diatoms and regions with variable iron inputs, as the storage protein could be critical in maintaining intracellular iron homeostasis in environments with rapidly changing external iron concentrations.

Structure, taxonomy, and phylogeny of diatom ferritin

The protein structure of ferritin may provide clues regarding its utilization in phytoplankton. The coastal marine diatom *P. multiseriis* has an isoform of ferritin that seems to be optimized for rapid iron sequestration and release. This diatom contains a glutamic acid residue in a region of the ferroxidase center (Glu130) that complexes and stabilizes Fe(III) following oxidation of Fe(II) (Pfaffen et al. 2015). This complexation reduces the rate of Fe(III) transfer to the protein core and subsequent storage as ferrihydrite. By contrast, substitution of Glu130 with a non-Fe coordinating residue allows for quicker Fe(III) mineralization and storage (Pfaffen et al. 2015). Interestingly, aside from *P. granii*, none of the other ferritin-containing diatoms examined in our study contain a glutamic acid or other iron-binding amino acid at site 130, but instead have an alanine, serine, or glycine (Supporting Information Fig. S6). In addition, all but one of these diatoms (*Thalassiosira* sp. NH16) have ferritins with gene expression patterns that differed compared to *P. multiseriis* (Marchetti et al. 2009) and *P. granii*, which was the only isolate to substantially increase *FTN* expression (by 100-fold) under high iron conditions in this study (Fig. 3B). The presence of glutamic acid in this key position at the ferroxidase center in *P. granii* is puzzling as its presence suggests a retarded transfer of Fe(III) between the ferroxidase site in ferritin and the site of ferrihydrite deposition, which one might argue would inhibit rather than facilitate long-term storage of iron. Clearly further work is needed to understand the ecological importance of these ferritin isoforms and whether differences in functional roles can result from minor variations in key amino acid residues in the ferroxidase centers.

Furthermore we report that taxonomically related diatoms contain ferritins with different expression patterns in cells grown under varying iron conditions. Variable ferritin expression patterns among diatom isolates is perhaps explained by multiple lateral gene transfer events or by gene mutation within the diatom lineage (Marchetti et al. 2009; Groussman et al. 2015). Within the *Thalassiosira* genus, *Thalassiosira* sp. NH16 significantly increased *FTN* expression under high iron conditions, while *T. rotula* contains one *FTN* gene where transcription significantly increased under low iron conditions and another with no change in expression. In addition *A. coffeaeformis* contains two *FTN* genes that are phylogenetically similar, yet display trends

similar to those observed in *T. rotula*. Given that closely related taxa may contain ferritins with different expression patterns, the functional roles of ferritins should not be based on taxonomic relatedness. In other words, ferritin functionality does not conform to diatom phylogeny.

Ferritin genes in *T. rotula* (*FTN2*) and *A. coffeaeformis* (*FTN1*) displayed similar gene expression responses to low iron conditions in which expression increased in one of two *FTN* genes; but there was substantial sequence variation between the species' ferritin proteins. In diatoms and other microalgae, there are two distinct clades of ferritins based on sequence homology in the C-terminus region. The subgroup with high bootstrap support (94%) and distinct sequence homology has been named FTN-II, whereas all other ferritins are known as FTN-I (see Fig. 1B; Groussman et al. 2015). Our findings suggest caution should be used in assuming that these phylogenetically determined clades could be used to predict a similarity in ferritin functional role within each clade. *P. granii* and *Thalassiosira* sp. NH16 both exhibit increased *FTN* expression under high iron conditions while *T. rotula* (*FTN2*) and *A. coffeaeformis* (*FTN1*) increased *FTN* expression under iron limiting conditions, yet all of these ferritins group within the FTN-I clade. Furthermore, as noted previously, a single residue substitution could substantially change ferritin functionality, suggesting that ferritin sequence homology alone may be an inaccurate indicator of ferritin function (Pfaffen et al. 2015).

Multiple roles for diatom ferritins

Gene expression patterns found in this study provide compelling support for multiple functional roles of ferritin among marine diatoms. One of these roles is for long-term storage during periods of high iron bioavailability, allowing for use of these iron reserves to support cell growth and division when iron in the surrounding environment drops back to low, growth-limiting concentrations. Such a role is consistent with the exceptionally large iron storage capacity and increasing *FTN* gene expression pattern observed at high Fe concentrations in *P. granii*, which also appear to be independent of light status or growth phase. Furthermore, *FTN* expression increases under high iron conditions in the diatom *Thalassiosira* sp. NH16, albeit to a much lower degree. These diatoms may have evolved ferritins specialized for long-term iron storage over multiple cell divisions.

For many of the diatom ferritins examined in this study there was no significant change in gene expression with variations in iron quota. These included those in the diatoms *M. polymorphus*, *T. rotula* (*FTN1*), *A. coffeaeformis* (*FTN2*), and *T. frauenfeldii* (*FTN1&2*). A similar pattern was observed in the green alga *O. tauri*, where *FTN* gene expression did not significantly change in response to iron limitation of growth, but rather was strongly regulated by diel cycles of light and photosynthetic carbon fixation (Botbol et al. 2015). Further studies investigating ferritin signaling pathways, regulation

factors, and ferritin localization under low iron conditions could provide a more comprehensive understanding of the mechanisms behind ferritin transcript regulation in these diatoms.

In contrast to *P. granii* and *Thalassiosira* sp. NH16, the diatoms *T. rotula* and *A. coffeaeformis* significantly increased expression of one of their two *FTN* genes under iron limitation of growth rate, suggesting that there is a role for ferritin under low iron conditions that may be widespread. One possibility may be as a proactive safety mechanism to protect cells against intracellular iron toxicity when high affinity iron uptake systems, which are upregulated under iron-limited growth (Shaked and Lis 2012), encounter pulses of iron. By utilizing ferritin as a short-term storage mechanism under low iron conditions, cells would be protected against possibly lethal doses of iron influx, and would be able to utilize the accumulated iron to support subsequent cellular growth. Alternatively, ferritins may need to store iron released from the cellular degradation of iron-containing proteins and protein complexes such as ferredoxin and photosystem I during cellular acclimation to low iron conditions (La Fontaine et al. 2002; Long et al. 2008). Further supporting the important role of ferritins in iron-limited cells, in ferritin knock-out experiments within the green alga *O. tauri*, cells without ferritin were less tolerant of low iron conditions than their wild-type counterparts (Botbol et al. 2015).

Increased expression of some ferritins under iron stress and the lack of decreased expression of many others under low iron conditions may reflect a necessary adaptation to inherent variations in iron supply and growth demand for cellular iron on a number of time-scales. There are inherent short-term changes in iron demand linked to diel variations in growth and light conditions due to vertical mixing and changing cloud cover (Sunda and Huntsman 2004). Likewise, iron availability can be quite variable on a number of time scales owing to photo-redox cycling of iron in sunlit surface waters and wind-driven changes in vertical mixing and upwelling of nutrient rich deeper waters (Sunda 2012).

Conclusion

This study aimed to examine whether ferritin-containing and non-containing centric and pennate diatoms systematically differ in their ability to store iron, and whether the two diatom lineages differ in their ferritin gene expression patterns as a function of iron status. Our findings demonstrate that centric diatoms can store iron to a similar extent as pennate diatoms with no clear relationship between the presence of ferritin and iron storage capacity in either lineage. However, the HNLC diatom *P. granii* demonstrated an exceptionally large iron storage capacity when compared to all other diatoms examined. We furthermore provide evidence to support multiple distinct functional roles for ferritin among diatoms, with the ferritin-containing diatoms *P.*

granii and *Thalassiosira* sp. NH16 increasing ferritin gene expression under high iron concentrations, consistent with a role in long-term iron storage. Conversely, two other diatoms species, *A. coffeaeformis* and *T. rotula*, contained two distinct ferritin genes where one increased in expression under iron limitation and the second showed no variation with cellular iron status. We conclude that diatom ferritin is a versatile protein for storing intracellular iron as needed to correct for temporal differences between cellular iron supply and metabolic demand on both short and long timescales. Thus it appears to be an integral protein for cellular function and is likely a contributing factor to the success of many diatoms in the marine environment.

References

- Alexander, H., B. D. Jenkins, T. A. Rynearson, M. A. Saito, M. L. Mercier, and S. T. Dyhrman. 2012. Identifying reference genes with stable expression from high throughput sequence data. *Front. Microbiol.* **3**: 385. doi:10.3389/fmicb.2012.00385
- Allen, A. E., and others. 2008. Whole-cell response of the pennate diatom *Phaeodactylum tricornutum* to iron starvation. *Proc. Natl. Acad. Sci. USA* **105**: 10438–10443. doi:10.1073/pnas.0711370105
- Altschul, S. F., W. Gish, W. Miller, E. W. Myers, and D. J. Lipman. 1990. Basic local alignment search tool. *J. Mol. Biol.* **215**: 403–410. doi:10.1016/S0022-2836(05)80360-2
- Armbrust, E. V. 2009. The life of diatoms in the world's oceans. *Nature* **459**: 185–192. doi:10.1038/nature08057
- Botebol, H., and others. 2015. Central role for ferritin in the day/night regulation of iron homeostasis in marine phytoplankton. *Proc. Natl. Acad. Sci. USA* **112**: 14652–14656. doi:10.1073/pnas.1506074112
- Bowler, C., and others. 2008. The *Phaeodactylum* genome reveals the evolutionary history of diatom genomes. *Nature* **456**: 239–244. doi:10.1038/nature07410
- Boyd, P. W., and others. 2007. Mesoscale iron enrichment experiments 1993 – 2005: Synthesis and future directions. *Science* **315**: 612–618. doi:10.1126/science.1131669
- Brand, L. E., R. R. L. Guillard, and L. S. Murphy. 1981. A method for the rapid and precise determination of acclimated phytoplankton reproduction rates. *J. Plankton Res.* **3**: 193–201. doi:10.1093/plankt/3.2.193
- de Baar, H. J. W., and others. 2005. Synthesis of iron fertilization experiments: From the iron age in the age of enlightenment. *J. Geophys. Res. C Oceans* **110**: 1–24. doi:10.1029/2004JC002601
- Edgar, R. C. 2004. MUSCLE: Multiple sequence alignment with high accuracy and high throughput. *Nucleic Acids Res.* **32**: 1792–1797. doi:10.1093/nar/gkh340
- Ellis, K. A., N. R. Cohen, C. Moreno, and A. Marchetti. 2017. Cobalamin-independent methionine synthase distribution and influence on vitamin B12 growth requirements in marine diatoms. *Protist* **168**: 32–47. doi:10.1016/j.protis.2016.10.007
- Garcia, H. E., R. A. Locarnini, T. P. Boyer, J. I. Antonov, M. M. Zweng, O. K. Baranova, and D. R. Johnson. 2010. World Ocean Atlas 2009, v. 4: Nutrients (phosphate, nitrate, silicate). In S. Levitus [ed.], NOAA Atlas. U.S. Government Printing Office.
- Groussman, R. D., M. S. Parker, and E. V. Armbrust. 2015. Diversity and evolutionary history of iron metabolism genes in diatoms. *PLoS One* **10**: e0129081. doi:10.1371/journal.pone.0129081
- Hillebrand, H., C.-D. Dürselen, D. Kirschtel, U. Pollinger, and T. Zohary. 1999. Biovolume calculation for pelagic and benthic microalgae. *J. Phycol.* **35**: 403–424. doi:10.1046/j.1529-8817.1999.3520403.x
- Keeling, P. J., and others. 2014. The Marine Microbial Eukaryote Transcriptome Sequencing Project (MMETSP): Illuminating the functional diversity of eukaryotic life in the oceans through transcriptome sequencing. *PLoS Biol.* **12**: e1001889. doi:10.1371/journal.pbio.1001889
- Kustka, A. B., A. E. Allen, and F. M. M. Morel. 2007. Sequence analysis and transcriptional regulation of iron acquisition genes in two marine diatoms. *J. Phycol.* **43**: 715–729. doi:10.1111/j.1529-8817.2007.00359.x
- La Fontaine, S., J. M. Quinn, S. S. Nakamoto, M. D. Page, V. Gohre, J. L. Moseley, J. Kropat, and S. Merchant. 2002. Copper-dependent iron assimilation pathway in the model photosynthetic eukaryote *Chlamydomonas reinhardtii*. *Eukaryot. Cell* **1**: 736–757. doi:10.1128/EC.1.5.736-757.2002
- Langar, V., and others. 2005. Mobilization of vacuolar iron by AtNRAMP3 and AtNRAMP4 is essential for seed germination on low iron. *EMBO J.* **24**: 4041–4051. doi:10.1038/sj.emboj.7600864
- LaRoche, J., H. Murray, M. Orellana, and J. Newton. 1995. Flavodoxin expression as an indicator of iron limitation in marine diatoms. *J. Phycol.* **31**: 520–530. doi:10.1111/j.1529-8817.1995.tb02545.x
- Liu, X., and E. C. Theil. 2005. Ferritins: Dynamic management of biological iron and oxygen chemistry. *Acc. Chem. Res.* **38**: 167–175. doi:10.1021/ar0302336
- Lommer, M., and others. 2012. Genome and low-iron response of an oceanic diatom adapted to chronic iron limitation. *Genome Biol.* **13**: R66. doi:10.1186/gb-2012-13-7-r66
- Long, J. C., F. Sommer, M. D. Allen, S.-F. Lu, and S. S. Merchant. 2008. FER1 and FER2 encoding two ferritin complexes in *Chlamydomonas reinhardtii* chloroplasts are regulated by iron. *Genetics* **179**: 137–147. doi:10.1534/genetics.107.083824
- Maldonado, M. T., and N. M. Price. 2001. Reduction and transport of organically bound iron by *Thalassiosira oceanica* (Bacillariophyceae). *J. Phycol.* **37**: 298–310. doi:10.1046/j.1529-8817.2001.037002298.x

- Marchetti, A., M. T. Maldonado, E. S. Lane, and P. J. Harrison. 2006. Iron requirements of the pennate diatom *Pseudo-nitzschia*: Comparison of oceanic (high-nitrate, low-chlorophyll waters) and coastal species. *Limnol. Oceanogr.* **51**: 2092–2101. doi:10.4319/lo.2006.51.5.2092
- Marchetti, A., and others. 2009. Ferritin is used for iron storage in bloom-forming marine pennate diatoms. *Nature* **457**: 467–470. doi:10.1038/nature07539
- Marchetti, A., and others. 2012. Comparative metatranscriptomics identifies molecular bases for the physiological responses of phytoplankton to varying iron availability. *Proc. Natl. Acad. Sci. USA* **109**: E317–E325. doi:10.1073/pnas.1118408109
- Marchetti, A., D. Catlett, B. M. Hopkinson, K. Ellis, and N. Cassar. 2015. Marine diatom proteorhodopsins and their potential role in coping with low iron availability. *ISME J.* **9**: 2745–2748. doi:10.1038/ismej.2015.74
- Marchetti, A., C. M. Moreno, N. R. Cohen, I. Oleinikov, K. DeLong, B. S. Twining, V. E. Armbrust, and R. H. Lampe. 2017. Development of a molecular-based index for assessing iron status in bloom-forming pennate diatoms. *J. Phycol.* **53**: 820–832. doi:10.1111/jpy.12539
- Moore, J. K., S. C. Doney, D. M. Glover, and I. Y. Fung. 2002. Iron cycling and nutrient-limitation patterns in surface waters of the World Ocean. *Deep-Sea Res. II* **49**: 463–507. doi:10.1016/S0967-0645(01)00109-6
- Moreno, C. M., Y. Lin, S. Davies, et al. 2017. Examination of gene repertoires and physiological responses to iron and light limitation in Southern Ocean diatoms. *Polar Biol.* 1–18. doi:10.1007/s00300-017-2228-7
- Morrissey, J., and C. Bowler. 2012. Iron utilization in marine cyanobacteria and eukaryotic algae. *Front. Microbiol.* **3**: 43. doi:10.3389/fmicb.2012.00043
- Morrissey, J., and others. 2015. A novel protein, ubiquitous in marine phytoplankton, concentrates iron at the cell surface and facilitates uptake. *Curr. Biol.* **25**: 364–371. doi:10.1016/j.cub.2014.12.004
- Nuester, J., S. Vogt, and B. S. Twining. 2012. Localization of iron within centric diatoms of the genus *Thalassiosira*. *J. Phycol.* **48**: 626–634. doi:10.1111/j.1529-8817.2012.01165.x
- Peers, G., and N. M. Price. 2006. Copper-containing plastocyanin used for electron transport by an oceanic diatom. *Nature* **441**: 341–344. doi:10.1038/nature04630
- Pfaffen, S., J. M. Bradley, R. Abdulqadir, M. R. Firme, G. R. Moore, N. E. Le Brun, and M. E. P. Murphy. 2015. A diatom ferritin optimized for iron oxidation but not iron storage. *J. Biol. Chem.* **290**: 28416–28427. doi:10.1074/jbc.M115.669713
- Pfaffl, M. W. 2001. A new mathematical model for relative quantification in real-time RT-PCR. *Nucleic Acids Res.* **29**: e45. doi:10.1093/nar/29.9.e45
- Price, N. M., G. I. Harrison, J. G. Hering, R. J. Hudson, P. M. V. Nirel, B. Palenik, and F. M. M. Morel. 1989. Preparation and chemistry of the artificial algal culture medium aquil. *Biol. Oceanogr.* **6**: 443–461. doi:10.1080/01965581.1988.10749544
- Raguzzi, F., E. Lesuisse, and R. R. Crichton. 1988. Iron storage in *Saccharomyces cerevisiae*. *FEBS Lett.* **231**: 253–258. doi:10.1016/0014-5793(88)80742-7
- Saito, M. A., A. E. Noble, A. Tagliabue, T. J. Goepfert, C. H. Lamborg, and W. J. Jenkins. 2013. Slow-spreading submarine ridges in the South Atlantic as a significant oceanic iron source. *Nat. Geosci.* **6**: 775–779. doi:10.1038/ngeo1893
- Sarmiento, J. L., and M. Bender. 1994. Carbon biogeochemistry and climate change. *Photosynth. Res.* **39**: 209–234. doi:10.1007/BF00014585
- Shaked, Y., A. B. Kustka, and F. M. M. Morel. 2005. A general kinetic model for iron acquisition by eukaryotic phytoplankton. *Limnol. Oceanogr.* **50**: 872–882. doi:10.4319/lo.2005.50.3.0872
- Shaked, Y., and H. Lis. 2012. Disassembling iron availability to phytoplankton. *Front. Microbiol.* **3**: 123. doi:10.3389/fmicb.2012.00123
- Sorhannus, U. 2007. A nuclear-encoded small-subunit ribosomal RNA timescale for diatom evolution. *Mar. Micropaleontol.* **65**: 1–12. doi:10.1016/j.marmicro.2007.05.002
- Strzepek, R. F., and P. J. Harrison. 2004. Photosynthetic architecture differs in coastal and oceanic diatoms. *Nature* **431**: 689–692. doi:10.1038/nature02954
- Sunda, W. G. 2012. Feedback interactions between trace metal nutrients and phytoplankton in the ocean. *Front. Microbiol.* **3**: 204. doi:10.3389/fmicb.2012.00204
- Sunda, W. G., and S. A. Huntsman. 1995. Iron uptake and growth limitation in oceanic and coastal phytoplankton. *Mar. Chem.* **50**: 189–206. doi:10.1016/0304-4203(95)00035-P
- Sunda, W. G., and S. A. Huntsman. 1997. Interrelated influence of iron, light and cell size on marine phytoplankton growth. *Nature* **390**: 389–392. doi:10.1038/37093
- Sunda, W. G., and S. A. Huntsman. 2004. Relationships among photoperiod, carbon fixation, growth, chlorophyll a, and cellular iron and zinc in a coastal diatom. *Limnol. Oceanogr.* **49**: 1742–1753. doi:10.4319/lo.2004.49.5.1742
- Tamura, K., G. Stecher, D. Peterson, A. Filipinski, and S. Kumar. 2013. MEGA6: Molecular Evolutionary Genetics Analysis version 6.0. *Mol. Biol. Evol.* **30**: 2725–2729. doi:10.1093/molbev/mst197
- Tang, D., and F. M. M. Morel. 2006. Distinguishing between cellular and Fe-oxide-associated trace elements in phytoplankton. *Mar. Chem.* **98**: 18–30. doi:10.1016/j.marchem.2005.06.003
- Theil, E. C., M. Matzapetakis, and X. Liu. 2006. Ferritins: Iron/oxygen biominerals in protein nanocages. *JBIC J.*

- Biol. Inorg. Chem. **11**: 803–810. doi:[10.1007/s00775-006-0125-6](https://doi.org/10.1007/s00775-006-0125-6)
- Theil, E. C., X. S. Liu, and T. Tosha. 2008. Gated pores in the ferritin protein nanocage. *Inorganica Chim. Acta* **361**: 868–874. doi:[10.1016/j.ica.2007.08.025](https://doi.org/10.1016/j.ica.2007.08.025)
- Twining, B. S., S. B. Baines, N. S. Fisher, and M. R. Landry. 2004. Cellular iron contents of plankton during the Southern Ocean Iron Experiment (SOFEX). *Deep-Sea Res. Part I Oceanogr. Res. Pap.* **51**: 1827–1850. doi:[10.1016/j.dsr.2004.08.007](https://doi.org/10.1016/j.dsr.2004.08.007)
- Untergasser, A., I. Cutcutache, T. Koressaar, J. Ye, B. C. Faircloth, M. Remm, and S. G. Rozen. 2012. Primer3—new capabilities and interfaces. *Nucleic Acids Res.* **40**: e115–e115. doi:[10.1093/nar/gks596](https://doi.org/10.1093/nar/gks596)

Acknowledgments

We thank anonymous reviewers for their careful review and helpful suggestions regarding our manuscript. We are grateful to the UNC Graduate School for providing partial doctoral funds to N.R.C. This research was funded through National Science Foundation (NSF) grant OCE1334935 to A.M. and NSF grant OCE1334632 to B.S.T. MMETSP was funded in part by the Gordon and Betty Moore Foundation through grant 2637 to the National Center for Genome Resources.

Conflict of Interest

None declared.

Submitted 12 June 2017

Revised 29 November 2017

Accepted 16 February 2018

Associate editor: James Moffett